Yuanansuchus maopingchangensis, the second capitosauroid temnospondyl from the Middle Triassic Badong Formation of Yuanan, Hubei, China

Jun Liu

The second species of *Yuanansuchus*, *Y. maopingchangensis*, is erected for new temnospondyl material from the Maopingchang site, Yuanan County, Hubei Province, China. These specimens are from a horizon approximately 20 m below the one that produced *Y. laticeps*, the first *Yuanansuchus* species to be described. *Y. maopingchangensis* shares the following features with *Y. laticeps*: tabular horn directed laterally; lateral line sulci continuous, well impressed; supraorbital sensory canal enters lacrimal; preorbital projection of jugal less than half length of snout; and vomerine plate short. However, *Y. maopingchangensis* differs from *Y. laticeps* in having an elongated skull, a frontal that may enter the medial border of the orbit and extend to the level of the posterior orbital margin, a closed otic fenestra, and a short cultriform process. Analysis of a new capitosaur phylogenetic data matrix, containing 56 characters and 29 species,confirms that the two species from Yuanan are sister taxa and that Capitosauroidea can bedivided into two major clades: one including *Parotosuchus*, *Eryosuchus*, *Calmasuchus* and *Cherninia*, and another including *Mastodonsaurus*, *Yuanansuchus*, *Stanocephalosaurus*, *Procyclotosaurus, Paracyclotosaurus, Antarctosuchus, Eocyclotosaurus*, *Quasicyclotosaurus*, *Tatrasuchus* and *Cyclotosaurus*.

Yuanansuchus maopingchangensis, the second capitosauroid temnospondyl from the Middle Triassic Badong Formation of Yuanan, Hubei, China

Jun Liu

Key Laboratory of Vertebrate Evolution and Human Origins of Chinese Academy of Sciences,

Institute of Vertebrate Paleontology and Paleoanthropology, Chinese Academy of Sciences

Beijing 100044, China

Abstract

A second species of *Yuanansuchus*, *Y. maopingchangensis*, is erected for new temnospondyl material from the Maopingchang site, Yuanan County, Hubei Province, China. These specimens are from a horizon approximately 20 m below the one that produced *Y. laticeps*, the first *Yuanansuchus* species to be described. *Y. maopingchangensis* shares the following features with *Y. laticeps*: tabular horn directed laterally; lateral line sulci continuous, well impressed; supraorbital sensory canal enters lacrimal; preorbital projection of jugal less than half length of snout; and vomerine plate short. However, *Y. maopingchangensis* differs from *Y. laticeps* in having an elongated skull, a frontal that may enter the medial border of the orbit and extend to the level of the posterior orbital margin, a closed otic fenestra, and a short cultriform process. Analysis of a new capitosaur phylogenetic data matrix, containing 56 characters and 29 species, confirms that the two species from Yuanan are sister taxa and that Capitosauroidea can be divided into two major clades: one including *Parotosuchus*, *Eryosuchus, Calmasuchus* and *Cherninia*, and another including *Mastodonsaurus*, *Yuanansuchus*, *Stanocephalosaurus*, *Procyclotosaurus*, *Paracyclotosaurus*, *Antarctosuchus*, *Eocyclotosaurus*, *Quasicyclotosaurus*,

Tatrasuchus and *Cyclotosaurus*.

INTRODUCTION

Temnospondyls are the largest and most speciose group of amphibians. Within this group, the stereospondyl clade Capitosauria produced some of the largest species and dominated many Mesozoic aquatic ecosystems (Schoch 2008). Capitosaur research has a long history, and more than 120 nominal species have been erected within this group (Damiani 2001; Fortuny et al. 2011; Liu & Wang 2005; Sidor et al. 2014; Sulej & Niedźwiedzki 2013). The taxonomy of Capitosauria was poorly understood for a long time, but recent systematic revisions of the group by Schoch & Milner (2000) and Damiani (2001) have led to a consensus regarding the taxonomic status of most previously named genera and species. Meanwhile, large-scale cladistic analyses of Capitosauria have been undertaken by Schoch (2000) and Damiani (2001). To resolve the position of *Yuanansuchus laticeps*, Liu and Wang (2005) added *Y. laticeps* and *Quasicyclotosaurus campi* to the matrix of Damiani (2001). In later works, researchers modified the character list and data matrix of Damiani (2001) for their own studies (Fortuny et al. 2011; Schoch 2008; Sidor et al. 2014), and they produced the phylogenetic hypotheses that have varied widely in such particulars as the position of *Edingerella*, the proximity of *Eryosuchus* to *Mastodonsaurus,* and the content of the subgroup Capitosauroidea (sensu Schoch, 2013) [figure 8 of Schoch (2008) vs. figure 7 of Fortuny et al. (2011)].

Capitosaurs are widely distributed on the land masses derived from the Pangean supercontinent, and are known from many good specimens (Damiani 2001; Schoch & Milner

2000). However, this group is poorly represented in east Asia (Ingavat & Janvier 1981; Li et al. 2008), a region from which only two highly informative capitosaur specimens have been described: the posterior part of a skull almost identical to the corresponding cranial region of *Cyclotosaurus posthumus* was reported from Thailand (Ingavat & Janvier 1981), and the nearly complete skull of a taxonomically novel capitosaur was reported from the Badong Formation of China. The notably broad Chinese skull was collected in Maopingchang Township, Yuanan County, Hubei Province in 2001, and was named *Yuanansuchus laticeps* (Liu & Wang 2005). In 2011 a mandibular fragment was reported from the Lower Triassic of Japan, implying that the dispersal of stereospondyls into China occurred before the latest Early Triassic (Nakajima & Schoch 2011).

In 2011, we made a second field trip to the Maopingchang locality and collected a considerable number of fossils. In this paper, several new temnospondyl specimens are described and assigned to a new species, *Yuanansuchus maopingchangensis*. *Y. maopingchangensis* represents the second temnospondyl species from Maopingchang. To evaluate the phylogenetic relationships of Chinese capitosauroids, a new character list is established based on a revision of previously established characters, and new matrices including both *Y. laticeps* and *Y. maopingchangensis* are constructed.

GEOLOGICAL SETTING

Outcrops of the Triassic Badong Formation are widely distributed in Hubei, Chongqing, and Hunan. The Badong Formation conformably overlies Lower Triassic shallow marine carbonates of the Jialinjiang Formation, and in most places underlies an Upper Triassic terrestrial coal series.

The Badong Formation is generally divided into five members, and vertebrate fossils have been collected from the purplish-red calcareous siltstone and mudstone of Member II in both Hunan and Hubei (Liu & Wang 2005; Zhang 1975). Member I contains a rich bivalve fauna, which is generally regarded Anisian in age. Member III yields the bivalves *Plagiostoma striatum* and *Placunopsis plana*, the ammonoid *Progonoceratites*, and the conodont *Neospathodus kockeli*, and is accepted as Anisian in age although Zhang et al. (2003) argued that it could instead be Ladinian. Member II has also been suggested to be Anisian in age, based on its fossil flora (Meng et al. 1995), so the fossil tetrapods from Member II are accepted here as Anisian. Member II has been interpreted as comprising tidal flat sediments (Meng et al. 1995), but the sediments at the Maopingchang locality are more likely to represent a floodplain facies. No tidal-related structures were observed in the field.

The specimens described in this paper were excavated from a hill 400 m away from the site of the holotype of *Yuanansuchus laticeps*, and from a stratigraphic level approximately 20 m lower in the section (Fig. 1). Among the bones collected at this spot, four skulls, one left lower jaw, three interclavicles, and nine clavicles are of temnospondyl origin. They represent at least six individuals, based on the number of clavicles. In addition to the temnospondyl fossils, vertebrae with high neural spines are present on the hill where *Y. maopingchangensis* was discovered, and almost certainly belong to an archosaur similar to *Lotosaurus* from Member II of the Badong Formation of Sangzhi County in Hunan (Zhang 1975).

Methods—The electronic version of this article in Portable Document Format (PDF) will represent a published work according to the International Commission on Zoological

Nomenclature (ICZN), and hence the new names contained in the electronic version are effectively published under that Code from the electronic edition alone. This published work and the nomenclatural acts it contains have been registered in ZooBank, the online registration system for the ICZN. A ZooBank LSID (Life Science Identifier) can be resolved and the associated information viewed through any standard web browser by appending the LSID to the prefix http://zoobank.org/. The LSID for this publication is: urn:lsid:zoobank.org:pub: D68F2D09-0AC0-4AE1-ACE1-EFD0C5680916. The online version of this work is archived and available from the following digital repositories: PeerJ, PubMed Central and CLOCKSS.

Abbreviation—IVPP, Institute of Vertebrate Paleontology and Paleoanthropology, Chinese Academy of Sciences, Beijing, China.

SYSTEMATIC PALEONTOLOGY

TEMNOSPONDYLI Zittel, 1887–1890

STEREOSPONDYLI Zittel, 1887–1890

CAPITOSAURIA Yates and Warren, 2000, sensu Schoch, 2008

CAPITOSAUROIDEA Säve-Söderbergh, 1935 sensu Schoch, 2013

Yuanansuchus Liu and Wang, 2005

Revised diagnosis—Tabular horn directed laterally; lateral line sulci continuous, well impressed; supraorbital sensory canal enters lacrimal; preorbital projection of jugal shorter than half length of snout; vomerine plate short; interclavicle wider than long; ventral part of blade of clavicle with convex medial margin.

Yuanansuchus maopingchangensis sp. nov.

Etymology—From "Maopingchang", the name of a village near the quarry.

Holotype—IVPP V 22628, a nearly complete skull.

Type Locality and Horizon—Maopingchang, Yuanan County, Hubei Province, China; Member II of the Badong Formation, Anisian, Middle Triassic.

Diagnosis—Differs from *Y. laticeps* in having an elongated skull, a large orbit, a closed otic notch, a frontal that barely contribute to the border of the orbit and extend to the level of the posterior orbital margin, and a short cultriform process of the parasphenoid that extends only to the anterior border of the interpterygoid vacuity.

Referred specimens: IVPP V 22629, a nearly complete skull; IVPP V 22630, an incomplete skull; IVPP V 22631, an incomplete left lower jaw; IVPP V 22632, a right clavicle articulating with the interclavicle; IVPP V 22633.1-2, two interclavicles; IVPP V 22634.1-8, eight clavicles including at least five right ones.

Description

The following description, except where specified otherwise, is based on the holotype; the other two known skulls are used as a supplemental source of information.

The holotype is a slightly distorted skull missing the posterolateral corner of the right cheek (Fig. 2). As preserved, the skull has an anteroposterior midline length of 275 mm and a width of 215 mm, but the complete skull was probably about 23 cm wide. This skull is slightly longer than IVPP V 13463, the holotype of *Yuanansuchus laticeps*, but is also much narrower. The posterior part of the skull was exposed and damaged by weathering prior to excavation of the rest of the specimen, so that the occipital and otic regions are poorly preserved. The skull roof is

127 generally well preserved, but white plaster has been inserted between the skull roof and palate to
128 reinforce the skull. None of the marginal or palatal teeth is preserved.

129 In dorsal and ventral views, the outline of the skull is parabolic and elongate, with straight
130 lateral margins. The outline is very similar to that of the skull of *Quasicyclotosaurus campi*
131 (Schoch 2000). The preorbital region is low in profile and relatively broad. The two sides of the
132 skull are asymmetrical. This anomaly can only partly be explained by distortion, and it seems
133 likely that the preserved shape is similar to the original one. The midline suture between the
134 frontals lies considerably further to the left than that between the nasals, so that the left nasal has
135 a substantial contact with the right frontal. In most capitosaurs, the midline is nearly straight.
136 Other differences in suture pattern exist between the left and right sides of the skull; for example,
137 the right frontal is distinctly longer than the left one.

138 The dermal sculpturing is well preserved on the skull roof (Fig. 2) and largely consists of a
139 pattern of deep pits, which grade into alternating ridges and grooves near the lateral margins of
140 the skull and the nasal surface. The lateral line sensory sulci are continuous and obvious on the
141 skull roof. The infraorbital sulcus (IS) has a Z-shaped lacrimal flexure, extends backwards along
142 the lateral skull margin on the maxilla, and seems continuous with the jugal sulcus (JS) to the
143 squamosal. The supraorbital sulcus (SS) is better-defined than the IS, runs across the prefrontal
144 and the lacrimal, nearly contacts the IS, and extends onto the nasal. The SS seems to not meet its
145 counterpart across the midline within the premaxilla. Posteriorly, the SS extends across the
146 frontal and postfrontal, and intersects with the temporal sulcus (TS) on the postorbital. The TS
147 extends downwards on the jugal to meet the IS, and extends posteriorly onto the supratemporal.

148 Skull Roof

149 A small interpremaxillary foramen lies on the midline, close to the anterior border of the
150 premaxillae. The nares are elongated and large (the left measuring 314 mm in length, and the
151 right 275 mm), and are situated near the anterior margin of the skull. The external naris is
152 bordered anteriorly and laterally by the premaxilla, dorsally by the nasal, and posteriorly by the
153 maxilla. The posterolaterally directed suture between the premaxilla and the nasal touches the
154 medial margin of the external naris, and the right suture is displaced anteriorly relative to the left
155 one. In dorsal view, the maxilla is restricted to the skull margin and does not extend posterior to
156 the anterior margin of the orbit. No septomaxilla is evident. The nasal contacts the maxilla pos-
157 terior to the external naris. The lacrimal contacts neither the orbit nor the naris.

158 The two large orbits are both ovoid, but differ in size, the right orbit being longer (43 mm in
159 length) and more anteriorly positioned than the left (38 mm in length). However, both orbits are
160 situated relatively far anteriorly, lying close to the mid-length of the skull roof. In this
161 characteristic *Y. maopingchangensis* resembles *Y. laticeps* and *Mastodosaurus giganteus*, but
162 differs from many other taxa (Liu & Wang 2005; Schoch 1999). The orbits are almost dorsally
163 directed and are raised above the rest of the skull roof, indicating an aquatic or semiaquatic
164 lifestyle in which the animal habitually positioned itself near the water surface. The highest point
165 on the skull roof is located on the postfrontal, just posterior to the orbit. The prefrontal is
166 relatively long (measuring about one quarter of the midline length of the skull), tapers to an
167 anterior point, and is elevated just anterior to the orbit. The frontal participates in the orbital
168 margin, as is the case in many other capitosaurs (Damiani 2001; Schoch 2008) but not in *Y.*

laticeps (Liu & Wang 2005). The frontal is subequal in length to the nasal, although the left frontal is shorter than the right. However, in contrast to the condition in all other capitosaurs, the frontal extends posteriorly beyond the posterior margin of the orbit (Schoch 2008; Schoch & Milner 2000). The postfrontal is a nearly quadrangular bone, and forms the posteromedial margin of the orbit. The postorbital is wide, and its lateral margin extends beyond that of the orbit. However, the postorbital does not extend as far anterolaterally as in many other capitosaurs, but narrows anteriorly and makes only a small posterior contribution to the orbital margin. The jugal forms most of the lateral border of the orbit, and has a long anterior process that extends far anterior to the orbit and reaches nearly the same level as the tip of the prefrontal. However, the length of the preorbital part of the jugal is nevertheless less than half that of the snout. Although the suture between the jugal and quadratojugal is unclear, the former is definitely the longest bone in the skull roof.

The parietal foramen is round and small, with a diameter of 6.5 mm, and lies on the midline near the anteroposterior midpoint of the parietals. The parietal is short, and is similar in length to the postparietal, the supratemporal, and the tabular. The postparietal is relatively long, its length exceeding its width. The posterior margin of the parietal is incompletely preserved but is nearly transversely aligned as in *Y. laticeps* and *Mastodonsaurus giganteus* (Liu & Wang 2005; Schoch 1999). The tabular is short and wide, and its lateral process is only slightly posteriorly directed. As a result, the posterior margin of the skull roof is nearly straight in dorsal view as in *Y. laticeps*, rather than distinctly concave as in most capitosaurs (Schoch 2008). The tabular contacts the squamosal, enclosing an otic fenestra and preventing the supratemporal from entering the dorsal

margin of this opening. The otic fenestra embays the squamosal more deeply than the tabular. The squamosal is a large bone in the posterolateral part of the skull roof. The posterior margin of the squamosal is poorly preserved, but this bone clearly does extend far enough posteriorly to overhang the occiput. The posterior margin of the postparietal, tabular andsquamosal appears thick (~7 mm) relative to the total height of the occiput (47 mm).

Palate

The palate is moderately vaulted, with the lateral edges slightly below the level of the middle portion. The maxilla bears many marginal tooth sockets, but no teeth are preserved. The paired anterior palatal vacuities are oval in outline and completely separated by the premaxilla and the vomer, as in *Mastodonsaurus giganteus* (Schoch 1999). A small fossa lies on the midline, crossing the suture between the premaxilla and the vomer. This structure may be a fossa subrostralis media, a feature present in *Eocyclotosaurus woschmidti* (Kamphausen 1989).

The vomerine plate is longer than wide. The plate is in contact with the premaxilla anteriorly, the maxilla laterally, and the palatine posterolaterally, and it sends out a long posteromedial process that runs lateral to the cultriform process. The vomerine tusk pair is large, and situated at the anterolateral corner of the vomer. The transvomerine tooth row is not preserved, but the protruding base shows it is slightly convex posteriorly. The left side of the plate is poorly preserved, but on the right side a depression is situated posterior to the transvomerine tooth row.

The choana is elliptical in outline, and relatively long. It is bordered by the maxilla laterally, the vomer medially, and the palatine posteriorly. The interpterygoid vacuities are well-developed,

measuring nearly 50% of the midline length of the skull, and are approximately as wide posteriorly as anteriorly. Each vacuity is bordered laterally by the palatine and pterygoid, and medially by the vomer and parasphenoid. The orbits are located at the level of the posterior half of the vacuities. Apart from a small portion of the right orbit, they can be seen through the vacuities in their entirety.

The palatine forms a slender posterior process that meets the ectopterygoid laterally and the pterygoid posteriorly. The palatine tusk pair is not preserved, and even the shapes of their alveoli are unclear. The right ectopterygoid is a slender triangular bone situated medial to the maxilla. However, the part of the palate forming the lateral margin of the left interpterygoid vacuity is so mediolaterally compressed that even the suture between the maxilla and the ectopterygoid is unclear.

Although the middle portion of the vomerine plate is not well-preserved, the length of the midline suture between the two vomers shows that the parasphenoid extends anteriorly to around the level of the anterior margin of the interpterygoid vacuities. The anterior tip of the parasphenoid is far more posteriorly positioned than in most capitosaurians, including *Y. laticeps*. The parasphenoid seems smoothly sutured with the vomer, and the fodina vomeralis should be absent here. The cultriform process is a flat bar which narrows laterally in the vicinity of its midpoint, and whose triangular base is smoothly continuous with the vaulted basal plate of the parasphenoid. The width of the basal plate is subequal to its length. The crista muscularis is a transversely oriented ridge located on the posterior rim of the basal plate. The ventrally positioned ‘pockets’ mentioned by Watson (1962) are indistinct and widely separated. The

232 parasphenoid contacts the pterygoid laterally at an anteroposteriorly long suture, the length of the
233 suture is slightly greater than the width of the corpus of the parasphenoid.
234 The palatine ramus of the pterygoid tapers anteriorly, and contacts the posterior margin of
235 the palatine along a short suture located roughly at the level of the anterior margin of the orbit.
236 The corpus of the pterygoid curves ventrally towards its lateral side; its lateral margin is granular
237 and forms a roughened area. The quadrate ramus has an oblique surface, and extends
238 posterolaterally to form a sutural contact with the main body of the quadrate. The palatine and
239 quadrate rami of the pterygoid participate in medially delimiting the subtemporal fenestra, which
240 is bordered posteriorly by the quadrate and laterally by the quadratojugal and maxilla. Both
241 quadrates are preserved. This bone is nearly triangular in palatal view, and the medial side which
242 contacts the pterygoid is much wider than the lateral side which contacts the quadratojugal. The
243 ventral condyle for the articular is saddle-like. The quadrate bears a boss (hyoid tubercle) above
244 the medial part of the condyle. The occipital condyles are separated from one another and are
245 formed by the exoccipitals, which are in sutural contact with the parasphenoid anteriorly. The
246 occipital condyles are positioned posteriorly to the level of the quadrate condyles. A long,
247 slender, unidentified piece of bone is preserved on the left ventral margin of the skull. The
248 anterior end of this unidentified element covers the posterior portion of the upper alveolar row.
249
250 The skull of IVPP V 22629 is nearly complete, with a midline length of 21 cm and a width
251 of approximately 15 cm (Fig. 3). The long axis of the orbit measures 27 mm, and the short axis
252 measures 20 mm. Another skull (IVPP V 22630) is slightly smaller (Fig. 4). Both specimens are

253 similar to the holotype in their general features, but differ from the holotype in that the frontal
254 merely comes close to the orbit rather than entering the orbital margin. The frontal extends only
255 to the level of the posterior margin of the orbits, rather than continuing posteriorly beyond this
256 level as in the holotype. In IVPP V 22629, only one vomerine tusk socket lies anterior to the
257 choana, and there is no socket lying posterior to the choana (Fig. 3B). In IVPP V 22629, the area
258 of the contact between the vomer and the cultriform process is poorly preserved, and the anterior
259 extent of the cultriform process is uncertain.

260 The occipital region is preserved in two specimens. The posttemporal fenestra is triangular.
261 The occipital condyle is poorly preserved, and is situated at the same dorsoventral level as the
262 quadrate condyle. The foramen magnum is low and wide. The right stapes is preserved in situ in
263 both specimens, and the one in IVPP V 22630 is complete. The stapedial footplate is large, and
264 the stapedial shaft is slab-like as in *Tatrasuchus wildi* (Schoch 1997). The foramen for nerves
265 IX-X (the glossopharyngeal and the vagal nerves) is visible on the lateral side of the exoccipital.

266

267 Lower jaw

268 IVPP V 22631 is a robust and long left lower jaw, missing the anterior tip and the
269 postglenoid area (Fig. 4). The intact specimen is estimated to have measured 266 mm in length
270 and 65 mm in height. The lower jaw increases in height posteriorly until the posterior end of the
271 coronoid, then begins to decease in height on the lateral side of the adductor fossa. As a result,
272 the dorsal margin of the lateral wall of the adductor fossa is strongly convex. The lateral surface
273 of the angular shows well−developed radial ornamentations, which become less evident on the

274 postsplenial. A distinct mandibular sulcus extends posterodorsally across the lateral surface of
275 the angular, beginning at the ventral margin.

276 The dentary bears more than 20 tooth sockets, which are anteroposteriorly compressed. Only
277 two broken teeth are preserved on the dentary. The middle and posterior coronoids each bear a
278 single row of teeth, but only a few conical teeth are actually preserved. The medial side of the
279 postsplenial bears a small anterior Meckelian foramen, posterior to which is an additional tiny
280 foramen. The posterior Meckelian foramen is bordered by the postsplenial anteriorly and
281 ventrally, the prearticular dorsally, and the angular posteoventrally. It is ovate and much larger
282 than the anterior Meckelian foramen, but still far less than half as long as the adductor fossa. The
283 prearticular extends anteriorly beyond the anterior margin of the posterior Meckelian foramen,
284 and contacts the postsplenial below the posterior coracoid. The hamate process of the prearticular
285 is not complete, but still rises above the level of the glenoid fossa. Most of the glenoid facet lies
286 above the level of the dorsal surface of dentary.
287

288 Postcranial skeleton

289 Many complete isolated bones have been discovered at this locality, but only a limited
290 number have been successfully excavated because they are quite fragile and the matrix is very
291 hard. Among the elements that have been recovered, three interclavicles and nine clavicles have
292 been identified as temnospondyl in origin and tentatively referred to *Y. maopingchangensis* (see
293 Discussion).

294 The interclavicle is well preserved in IVPP V22632 (Fig. 5). It is rhomboidal in shape,

295 lacking a distinct anterior stylus, and is much wider than long. In contrast, the interclavicle is
296 longer than wide in *Mastodonsaurus giganteus* (Schoch 1999). On the dorsal side, this bone
297 bears three converging ridges (Figs. 5B, C). The anterior two ridges lie in the anteroposteriorly
298 middle portion of the bone, and the posterior one is longitudinally aligned. The anterior and
299 posterior margins of the interclavicle are broad and nearly straight. The ventral surface displays
300 the characteristic temnospondyl dermal sculpture pattern, with furrows and ridges radiating
301 outwards from a central point.

302 Among the nine clavicles, only two right clavicles are nearly complete (Fig. 5). The ventral
303 blade of the clavicle is slightly longer than wide, and shows a radial ornamentation on the ventral
304 surface. The medial margin is convex, making the blade fanlike in shape rather than triangular.
305 The dorsal process is posterodorsally directed and similar to that of *Eryosuchus pronus* (Damiani
306 2001; Howie 1970). The lateral surface of the dorsal process combines with the ventral blade to
307 form a prescapular cavity, and the dorsal process tapers to form a sharp dorsal tip.

308 DISCUSSION

309 The only previously reported tetrapod species from the Maopingchang locality is
310 *Yuanansuchus laticeps*. The specimen IVPP V 22628 is quite different from the only known
311 specimen of *Yuanansuchus laticeps*, and cannot be referred to this species. IVPP V 22628 differs
312 from *Yuanansuchus laticeps* in possessing the following features: elongated skull, large orbit,
313 frontal entering the medial border of the orbit, closed otic fenestra, and short cultriform process.
314 Particularly considering that IVPP V 22628 is similar in skull length to the holotype of *Y.*
315 *laticeps*, the differences between the two specimens are great in magnitude to represent

316 intraspecific variation, implying that IVPP V 22628 represents a new taxon. This specimen has a
317 laterally directed tabular horn, as in the holotype of *Y. laticeps*, and the lateral orientation of the
318 horn is a unique feature not known in other capitosaurs. Although such capitosaurs as
319 *Eryosuchus* and *Mastodonsaurus* have been described as having laterally directed tabular horns
320 (Damiani 2001; Schoch 2008), their tabular horns in fact differ from those of the two Chinese
321 taxa in being directed posterolaterally.

322 The two small skulls collected from the same small hill (IVPP V 22629, 22630) are very
323 similar to IVPP V 22628 in most features but differ in that the frontal is excluded from the
324 orbital margin in both specimens. As shown by Kamphausen (1994), however, frontal
325 asymmetry can be present even in a single skull, so these two specimens are referred to *Y.*
326 *maopingchangensis* here. The lower jaw and postcranial bones are tentatively also referred to *Y.*
327 *maopingchangensis* because they came from the same small hill where the skulls described in
328 this paper were found. All of the cranial material from this spot is referable to *Y.*
329 *maopingchangensis*. Because postcranial morphology is relatively stable within most small
330 temnospondyl clades, the postcranial features observed in the new Maopingchang specimens
331 probably characterize the entire genus *Yuanansuchus* rather than only *Y. maopingchangensis*.

332

333 Phylogenetic analysis

334 To assess the phylogenetic position of *Yuanansuchus maopingchangensis*, I incorporated
335 this taxon into the data matrices of Schoch (2008) and Sidor et al. (2014), both of which
336 represent modifications of that of Damiani (2001). The original dataset of Damiani (2001)

337 included 47 characters. Fortuny et al. (2011) analyzed a modified version of this matrix, which
338 excluded Damiani's (2001) characters 22 and 34 but added eight new characters. Subsequently,
339 Sidor et al. (2014) added *Antarctosuchus* to the matrix of Fortuny et al. (2011). When I ran the
340 matrix of Sidor et al. (2014) using the same software (PAUP 4.0 beta 1.0 for PC) (Swofford 2001)
341 and settings specified in the paper, the results differed from those reported by Sidor et al. (2014)
342 in that *A. polyodon* was found to be the sister taxon of *Mastodonsaurus giganteus* rather than that
343 of *Paracyclotosaurus crookshanki*, although the parameters two equally most parsimonious trees
344 were the same (145 steps, a consistency index of 0.40, and a retention index of 0.70). Except
345 with respect to the position of *Antarctosuchus*, however, the two trees are topologically identical
346 with each other and with the cladogram published by Fortuny et al. (2011). The two species of
347 *Yuanansuchus* were added to the dataset (see Supplemental Data), which was analyzed in Paup
348 4.0b10 using the same settings as before. This analysis recovered two most parsimonious trees,
349 the strict consensus of which is almost identical to figure 7B of Fortuny et al. (2011) except in
350 that *Antarctosuchus* appears as the sister taxon of *Mastodonsaurus* and the Chinese clade
351 comprising *Y. laticeps* and *Y. maopingchangensis* appears as the sister taxon of *Xenotosuchus*
352 *africanus*.

353 Schoch (2008) revised the characters of Damiani (2001) and added 19 further characters and
354 used slightly different list of taxa. He obtained results quite different from those of Fortuny et al.
355 (2011) and Sidor et al. (2014), one key difference being that *Edingerella* was recovered as a
356 trematosaur rather than a capitosaur by Schoch (2008). However, when Schoch's (2008) small
357 matrix of 25 taxa was analyzed in Paup 4.0b10, the shortest trees were found to be only 152 steps

358 long, whereas the single most parsimonious tree reported by Schoch (2008) was 162 steps. The
359 strict consensus of the trees obtained is similar to the topology depicted in Schoch's (2008)
360 figure 8, but includes the monophyletic clade (((*Cyclotosaurus* (*Eocyclotosaurus*,
361 *Quasicyclotosaurus*)), *Mastodonsaurus*), *Paracyclotosaurus*). The matrix of Schoch (2008)
362 including *Yuanansuchus laticeps* resulted in an unresolved strict consensus tree.

363 To resolve the interrelationships of Capitosauria, a new data matrix was constructed using a
364 revised list of 56 characters (Appendix 1). The codings of the characters were mostly adopted
365 from previous analysis, though the matrix incorporates a few novel codings based on
366 examination of specimens, photos and the literature (Table 1). *Y. maopingchangensis* was coded
367 primarily based on the holotype, and secondarily with reference to the other specimens described
368 in this study. The matrix was analyzed with Paup 4.0b10 (Swofford 2001) and TNT 1.1
369 (Goloboff et al., 2003), and all characters were equally weighted and left unordered. Each
370 program recovered the same two most parsimonious trees, which were 188 steps in length. One
371 tree (Fig. 6A) is similar in its basic pattern to that depicted in figure 7A of Fortuny et al. (2011).
372 Both topologies posit the two Chinese taxa as a monophyletic clade, supporting referral of the
373 new species to *Yuanansuchus*. The positioned recovered for this clade is more basal than that
374 recovered for *Y. laticeps* by Liu and Wang (2005) and Schoch (2008), but still falls on the branch
375 of capitosauroid phylogeny that includes *Cyclotosaurus*. Schoch (2013) defined Capitosauroidea
376 as the least inclusive clade containing *Parotosuchus nasutus* and *Cyclotosaurus robustus*. Here,
377 Capitosauroidea can be divided into two clades: a relatively small one containing *Parotosuchus*,
378 and a much larger one containing *Cyclotosaurus*. Capitosauroidea includes *Edingerella*,

379 *Watsonisuchus*, and *Xenotosuchus* in one most parsimonious tree (fig. 6A) but not in the other
380 (fig. 6B). In the phylogenies of Fortuny et al. (2011) and Sidor et al. (2014), *Parotosuchus* and
381 *Cyclotosaurus* are positioned close to one another, resulting in a restricted Capitosauroidea that
382 excludes *Paracyclotosaurus* and many other taxa recovered as capitosauroids in the present
383 analysis. The present analysis did not recover a close relationship between *Eryosuchus* and
384 *Mastodonsaurus*.

385 ## CONCLUSION

386 The new temnospondyl specimens collected from the Maopingchang site (Yuanan, Hubei,
387 China) are assigned here to a new capitosaur species, *Yuanansuchus maopingchangensis*. This
388 species is the second to be named from the site, and shares the following features with *Y. laticeps*:
389 tabular horn directed laterally; lateral line sulci continuous, well impressed; supraorbital sensory
390 canal enters lacrimal; preorbital projection of jugal less than half length of snout; and vomerine
391 plate short. *Y. maopingchangensis* differs from *Y. laticeps* in having the following characteristics:
392 elongated skull; large orbit; frontal that may enter medial border of orbit; closed otic fenestra;
393 and short cultriform process. A phylogenetic analysis confirms that the two species form a
394 monophyletic clade, and supports the existence of a major dichotomy between separate
395 *Parotosuchus* and *Cyclotosaurus* lineages within Capitosauroidea.

396

397 ## ACKNOWLEDGEMENTS

398 I thank my field team (LI Lu, JIA Zhenyan, LI Yan, XU Xu) for collecting the specimens,
399 WU Yong and FU Hualin for preparing the specimens, XU Yong for helping to illustrate the

paper. Corwin Sullivan kindly read the draft of this paper and significantly improved the language. Boris Morkovin (Borissiak Paleontological Institute, Moscow, Russia) kindly sent some photos and references.

REFERENCES

Damiani RJ. 2001. A systematic revision and phylogenetic analysis of Triassic mastodonsauroids (Temnospondyli: Stereospondyli). *Zoological Journal of the Linnean Society* 133:379-482.

Fortuny J, Galobart À, and De Santisteban C. 2011. A new capitosaur from the Middle Triassic of Spain and the relationships within the Capitosauria. *Acta Palaeontologica Polonica* 56:553-566.

Goloboff, P., Farris, J., Nixon, K.. 2003b. T.N.T.: Tree Analysis Using New Technology. Program and documentation, available at http://www.zmuc.dk/public/phylogeny/tnt.

Howie AA. 1970. A new capitosaurid labyrinthodont from East africa. *Palaeontology* 13:210-253.

Ingavat R, and Janvier P. 1981. *Cyclotosaurus* cf. *posthumus* Fraas (Capitosauridae, Stereospondyli) from the Huai Hin Lat Formation (Upper Triassic), Northeastern Thailand: With a note on capitosaurid biogeography. *Geobios* 14:711-725.

Kamphausen D. 1989. Der Schädel von *Eocyclotosaurus woschmidti* ORTLAM (Amphibia, Stegocephalia) aus dem Oberen Buntsandstein (Trias) des Schwarzwaldes (SWDeutschland). *Stuttgarter Beiträge zur Naturkunde, Serie B (Geologie und Paläontologie)* 149:1-65.

Kamphausen D. 1994. Eine Schädelasymmetrie bei Cyclotosaurus Fraas (Amphibia, Stegocephalia) aus dem Stubensandstein (Trias) von Württemburg (SW-Deutschland). *Stuttgarter Beiträge zur Naturkunde, Serie B (Geologie und Paläontologie)* 210:1-12.

Li J, Wu X, and Zhang F. 2008. The Chinese Fossil Reptiles and Their kin (second edition). Beijing: Science Press. p 473.

Liu J, and Wang Y. 2005. The first complete mastodonsauroid skull from the Triassic of China: *Yuanansuchus laticeps* gen. et sp. nov. *Journal of Vertebrate Paleontology* 25:725-728.

Meng F, Zhang Z, and Xu A. 1995. *Nonmarine biota and sedimentary facies of the Badong Formation in the Yangzi and its neighbouring areas*. Wuhan: China University of Geosciences Press.

Nakajima Y, and Schoch RR. 2011. The first temnospondyl amphibian from Japan. *Journal of Vertebrate Paleontology* 31:1154-1157.

Schoch RR. 1997. A new capitosaur amphibian from the Upper Lettenkeuper (Triassic: Ladinian) of Kupferzell (Southern Germany). *Neues Jahrbuch für Geologie und Paläontologie, Abhandlungen* 203:239-272.

Schoch RR. 1999. Comparative osteology of *Mastodonsaurus giganteus* (Jaeger, 1828) from the

Middle Triassic (Lettenkeuper: Longobardian of Germany (Baden-Württemberg, Bayern, Thürbingen). *Stuttgarter Beitrage zur Naturkunde - Serie B* 278:1-175.

Schoch RR. 2000. The status and osteology of two new cyclotosaurid amphibians from the Upper Moenkopi Formation of Arizona (Amphibia: Temnospondyli; Middle Triassic). *Neues Jahrbuch für Geologie und Paläontologie, Abhandlungen* 216:387-411.

Schoch RR. 2008. The Capitosauria (Amphibia): characters, phylogeny, and stratigraphy. *Palaeodiversity* 1:189-226.

Schoch RR. 2013. The evolution of major temnospondyl clades: an inclusive phylogenetic analysis. *Journal of Systematic Palaeontology* 11:673-705.

Schoch RR, and Milner AR. 2000. *Stereosondyli*. Munchen: Verlag Dr. Friedrich Pfeil.

Sidor CA, Steyer JS, and Hammer WR. 2014. A new capitosauroid temnospondyl from the Middle Triassic upper Fremouw Formation of Antarctica. *Journal of Vertebrate Paleontology* 34:539-548.

Sulej T, and Niedźwiedzki G. 2013. A new large capitosaur temnospondyl amphibian from the Early Triassic of Poland. *Acta Palaeontologica Polonica* 58:65-75.

Swofford, D.L. 2001. PAUP: Phylogenetic Analysis Using Parsimony, Version 4.0b10. Smithsonian Institution, Washington DC.

Watson DMS. 1962. The Evolution of the Labyrinthodonts. *Philosophical Transactions of the Royal Society of London Series B, Biological Sciences* 245:219-265.

Zhang F-K. 1975. A new thecodont Lotosaurus, from Middle Triassic of Hunan. *Vertebrata Palasiatica* 13:144-147.

Zhang W-T, Chen P-J, and Palmer AR. 2003. Biostratigraphy of China. Beijing: Science Press. p 603.

Table 1(on next page)

Data matrix

Table 1. Data matrix used in the phylogenetic analysis

Table 1. Data matrix used in the phylogenetic analysis

Angusaurus spp.	1111011111	0100111011	1121100010	0010011010	1111100000	100100
Benthosuchus sushkini	1100101101	0101110011	0110100011	0011011100	0011000000	100100
Calmasuchus acri	0101000?00	11?1?1?102	00001?1011	111????112	0011000001	011??1
Cherninis denwai	0101100200	1112010000	0000111011	11111111??	?????0000?	100010
Cyclotosaurus robustus	0101000200	1111001200	1010111111	1111111122	10???10110	002111
Edingerella madagascariensis	010010[01]200	1111100001	00001[01]1010	10010?1101	001?011000	000100
Eocyclotosaurus spp.	1101101201	0112111002	1110111111	1011111?2	?????10010	122111
Eryosuchus garjainovi	010110020[01]	111101110[01]	0000111011	1111111122	1011000101	000000
Lydekkerina huxleyi	0110000100	0101000002	0000100001	0010001010	0011000000	000000
Mastodonsaurus giganteus	0101001201	1101011102	1010111111	1111111122	1111000110	100011
Odenwaldia heidelbergensis	110010020?	?1110?0??2	????????1?	??111?11??	?????00???	100?1?
Paracyclotosaurus crooshkanki	0101100200	1112010102	100?111111	11111111??	?????1111?	11101?
Parotosuchus orenburgensis	0100100200	1112010100	0010111011	1111111111	0011000001	100100
Procyclotosaurus stantonensis	1101100200	111201100?	0???1??111	?1111111??	?????0111?	1[12]1?11
Quasicyclotosaurus campi	0101101201	0102101002	001011?111	10??011111	10???10110	122111
Rhineceps nyasaensis	0000000000	0001000000	0000000000	0000000100	0000000000	00010?
Tatrasuchus wildi	0101?00200	1111000200	0000111011	1111111111	1111010111	001111
Thoosuchus yakovlevi	1100011111	0100110012	0121100000	0010011000	1111100000	100100
Trematosaurus brauni	1110011111	0100111 0?2	1121???010	01100?1020	1111100000	100100
Stanocephalosaurus birdi	0101000200	1112011001	0001111111	1111111111	0011011011	111001
Stanocephalosaurus pronus	0101000200	1112011000	0001111111	1111?11111	00?1011010	111001
Uranocentrodon senekalensis	0000000000	0000000000	0000000001	0?00000100	0000000000	000000
Vladlenosaurus alexeyevi	1100100200	0110010010	01001?1011	1???????11	?11?000000	100111
Watsonisuchus spp.	0100100200	1112010010	0000111011	1011111111	0011011000	100100

Wetlugasaurus angustifrons	010010020[01]	0111010010	0100111011	0101111111	1011000000	100100
Xenotosuchus africanus	0101100200	1111011000	0000111011	11?1111111	0011011100	10010?
Antarctosuchus polyodon	0?0??012?0	11120?110?	10?0110111	10??1111??	???????10?	11?101
Yuanansuchus laticeps	0102101211	010100100?	0000111011	1?111111??	?????1100?	2010?1
Yuanansuchus maopingchangensis	0102101201	1101101002	0000111011	11?11111??	?????110??	102100
Yuanansuchus maopingchangensis	0102101201	[01]101101002	0000111011	11?11111?1	01110110??	102100

(The taxa in the matrix include all 26 species analyzed by Fortuny et al. (2011), plus *Antarctosuchus*, *Yuanansuchus laticeps* and *Y. maopingchangensis*. Codings for most species were adapted from Schoch (2008) and Fortuny et al. (2011), but codings for *Antarctosuchus* were adapted from (Sidor et al. 2014) and the two species of *Yuanansuchus* were coded based on personal observation of specimens. *Y. maopingchangensis* was coded primarily based on the holotype, and secondarily with reference to other known specimens. A few previous codings are revised here based on photos and the literature. For example, character 16 was coded as (1) in *Antarctosuchus* by Sidor et al. (2014), but the reconstruction presented by these authors would actually suggest a coding of (0). In the present matrix a coding of (?) is adopted because the relevant part of the specimen is poorly preserved.)

1

fossil locality

Figure 1. The fossil locality at Maopingchang Township, Yuanan County, Hubei Province, China. All described specimens can from this locality, and the blue arrow points to the place of the holotype. Photo shot by the author.



Figure 2(on next page)

Photos and drawings of holotype

Figure 2. Photos and drawings of holotype of *Yuanansuchus maopingchangensis* sp. nov. (IVPP V 22628) in (A) dorsal and (B) ventral views. Abbreviations: apv, anterior palatal vacuity; ch, choana; cmp, crista muscularis of parasphenoid; cp, cultriform process of the parasphenoid; Ec, ectopterygoid; Eo, exoccipital; F, frontal; fsm, fossa subrostralis media; ipf, interpremaxillary foramen; is, infraorbital sulcus; J, jugal ; js, jugal sensory canal; L, lacrimal; lf, lacrimal flexure; M, maxilla; N, nasal; P, parietal; Pl, palatine; Po, postorbital; Pof, postfrontal; Pp, postparietal; Prf, prefrontal; Ps, parasphenoid; Pt, pterygoid; Q, quadrate; Qj, quadratojugal; spt, socket of palatine teeth; Sq, squamosal; ss, supraorbital sulcus; St, supratemporal; svt, socket of vomerine teeth; T, tabular; ts, temporal sulcus; V, vomer.

PeerJ Manuscript to be reviewed

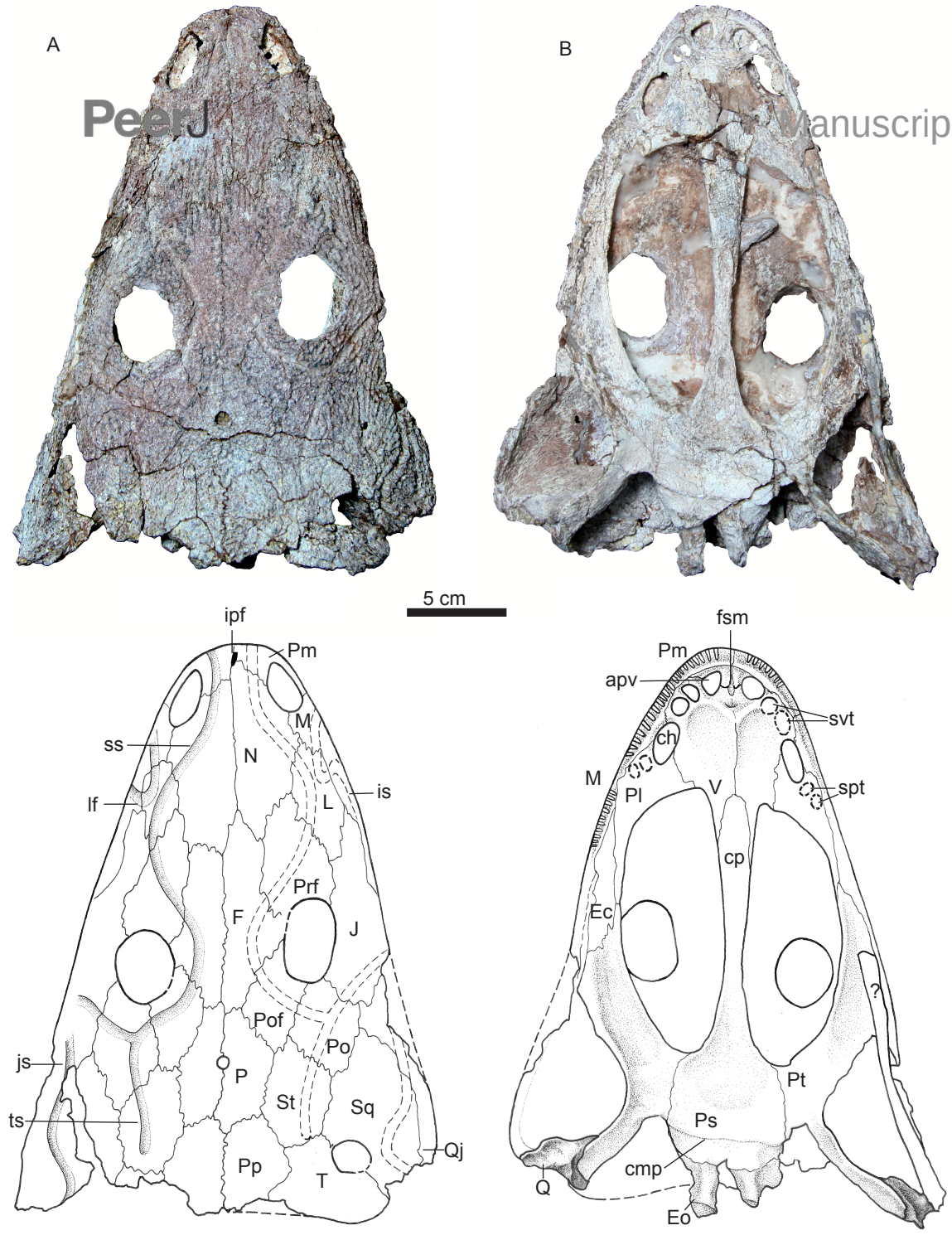


Figure 3(on next page)

Skull of IVPP V 22629

Figure 3. Skull of *Yuanansuchus maopingchangensis* sp. nov. (IVPP V 22629) in (A) dorsal, (B) ventral and (C) occipital views.

PeerJ Manuscript to be reviewed

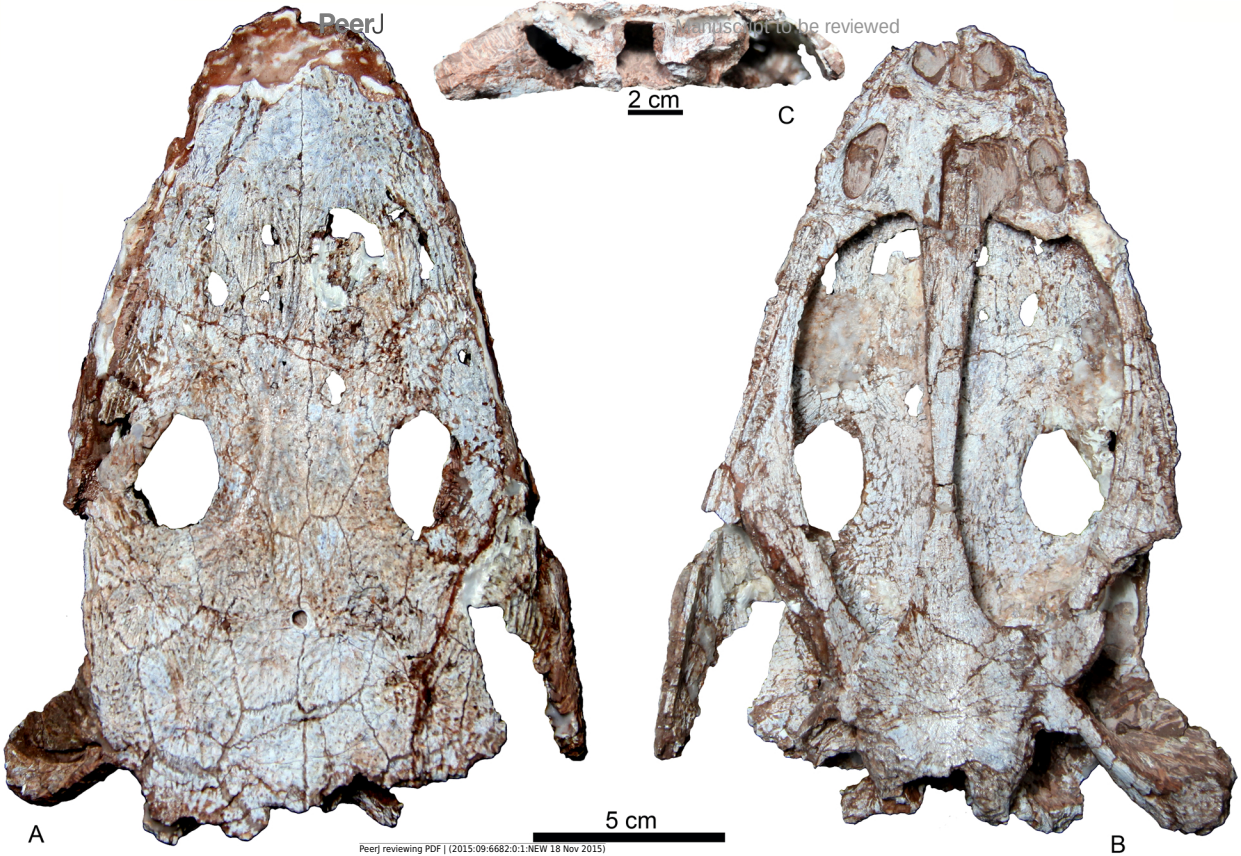


Figure 4(on next page)

Skull of *Yuanansuchus maopingchangensis* sp. nov. (IVPP V 22630)

Figure 4. Skull of *Yuanansuchus maopingchangensis* sp. nov. (IVPP V 22630) in (A) dorsal and (B) occipital and (C) posterolateral views; lower jaw (IVPP V 22631) in (D) lateral, (E) medial and (F) dorsal views. A, angular; af, adductor fossa; Art, articular; amf, anterior meckelian foramen; D, dentary; Eo, exoccipital; f.ix-x, foramen for glossopharyngeal and vagal nerves; gf, glenoid fossa; hp, hamate process of the prearticular; Mc, middle coronoid; ms, mandibular sulcus; Par, preaticular; Pc, posterior coronoid; pmf, posterior meckelian foramen; Psp, postplenial; ptf, posttemporal fenestra; S, stapes; Sa, surangular; Sp, splenial; T, tabular; t, tooth.

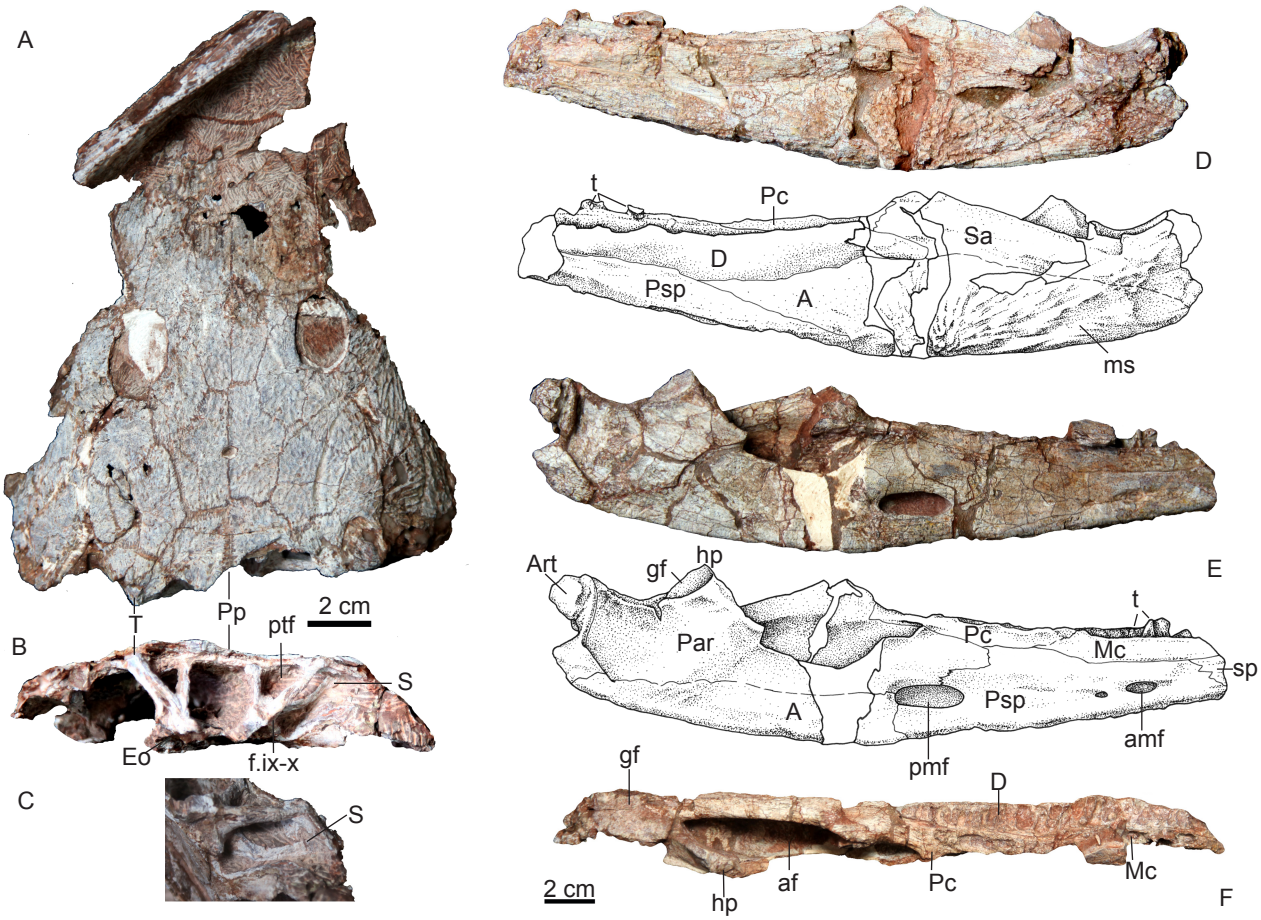

A
T
Pp
ptf
2 cm
B
S
Eo
f.ix-x
C
S
D
t
Pc
Sa
D
Psp
A
ms
E
Art
gf
hp
t
Par
Pc
Mc
sp
A
Psp
amf
pmf
gf
D
Mc
2 cm
af
Pc
hp
F

Figure 5(on next page)

Interclavicle and right clavicle

Figure 5. Interclavicle and right clavicle of *Yuanansuchus maopingchangensis* sp. nov. (IVPP V 22632) in (A) ventral and (B) dorsal views; (C) interclavicle (IVPP V 22633.1) in ventral view; right clavicle (IVPP V 22634.1) in (D) ventral and (E) dorsal views. Photo A was shot in the field.

PeerJ
Manuscript to be reviewed

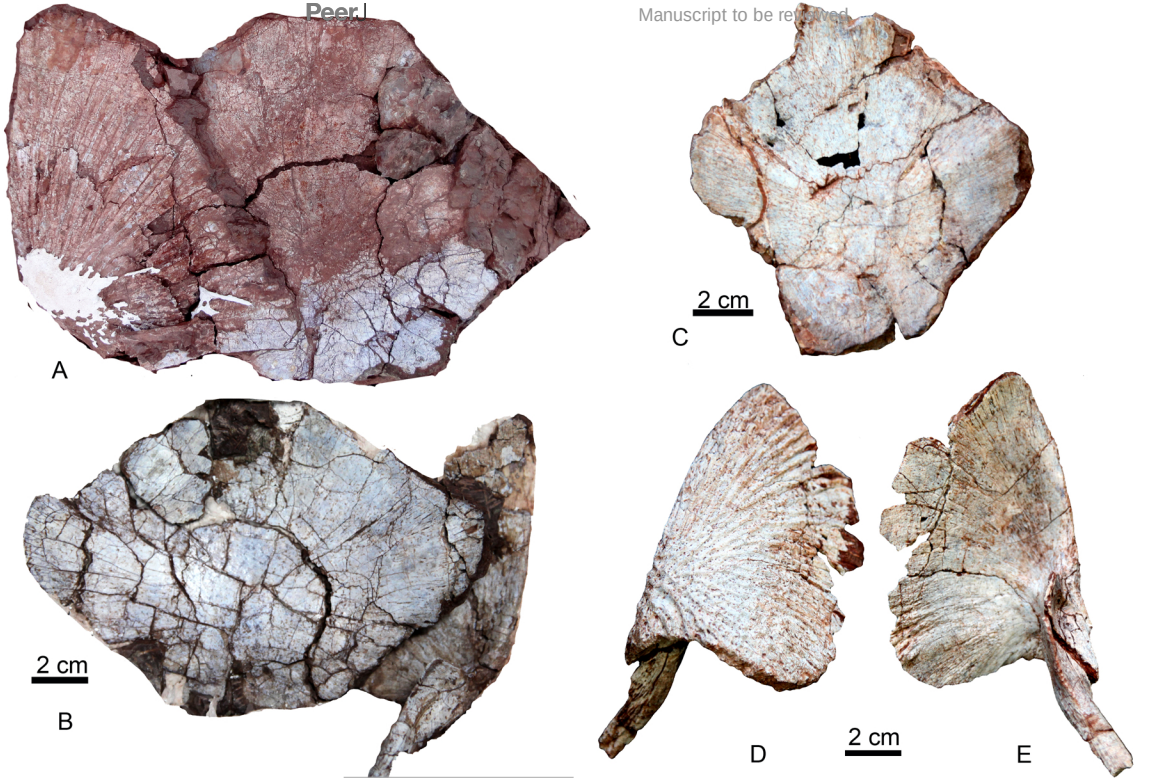
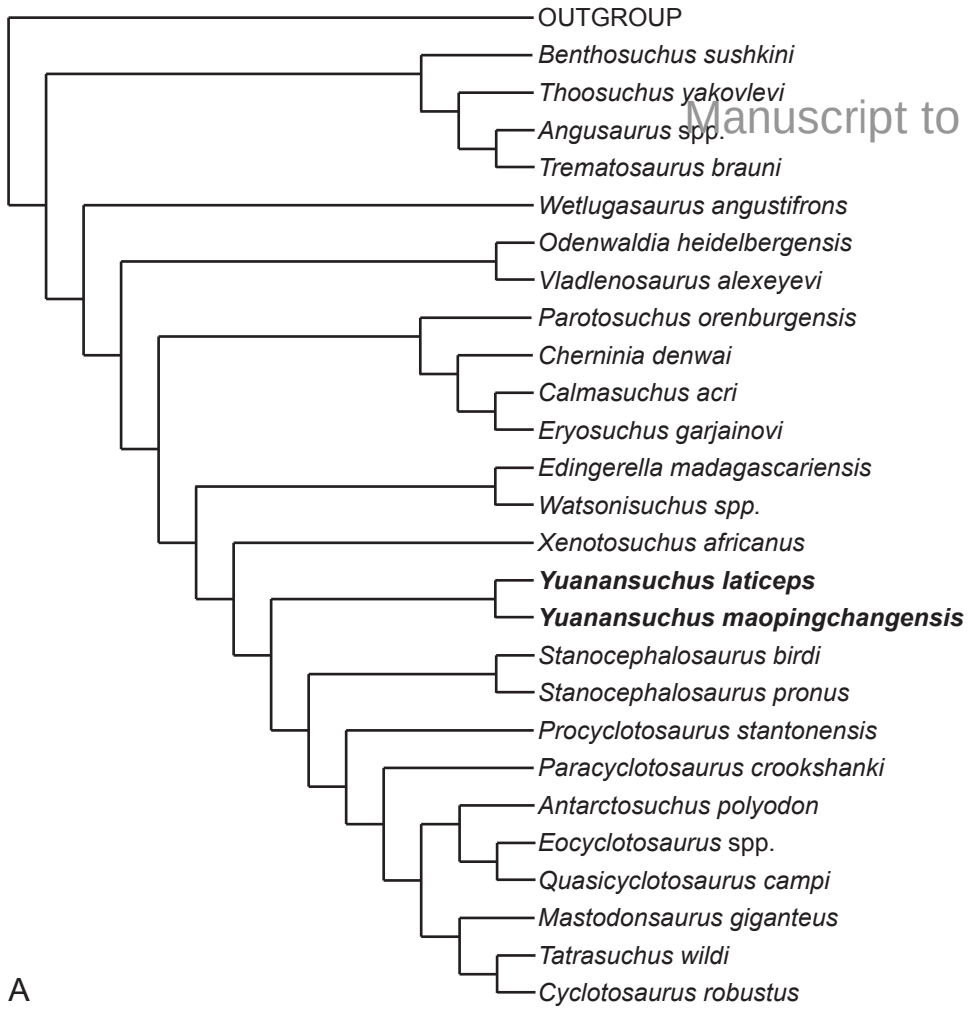


Figure 6(on next page)

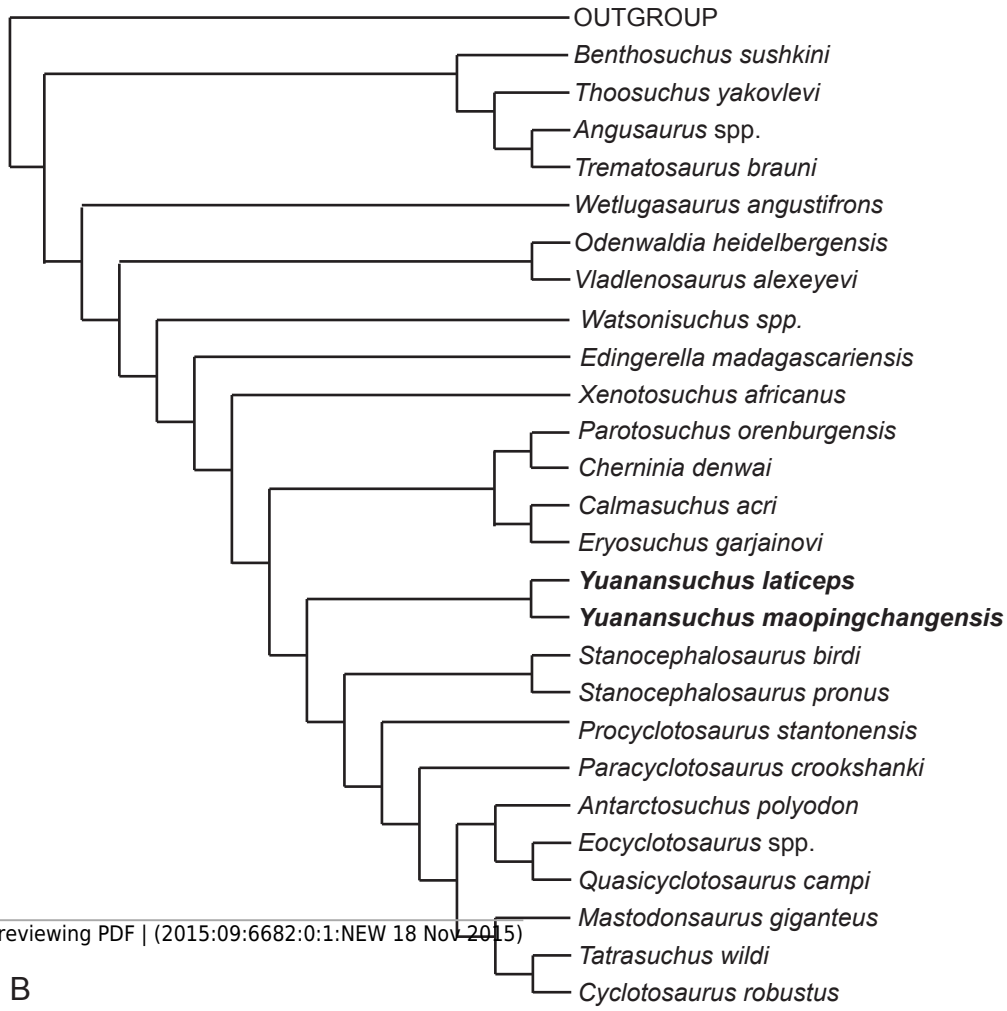
cladogram

Figure 6. Cladistic relationships of the capitosaurian temnospondyls, two most parsimonious trees recovered from a cladistic analysis of 29 taxa and 56 characters.

PeerJ Manuscript to be reviewed



A



B

Appendix 1 Character list

The following 57 characters were revised from the character lists of Schoch (2008) and Fortuny et al. (2011), both of them were derived from Damiani (2001). The following abbreviations are used here: D, Damiani (2001); S, Schoch (2008); F, Fortuny et al. (2011). The number following the abbreviation indicates the position of the character in the author's list. Italics indicate that the definition of the character provided by the previous author(s) differs from that provided here.

1. **Preorbital region**. Parabolic (0), or tapering (1). [*D1*, S1, *F1*]

2. **Posterolateral skull corners (quadrates)**. Posterior to distal end of tabular horns (0), or anterior (1). [D2, S2, F2]

3. **Otic notch**. Deeply incised into posterior skull margin (0), or reduced to an embayment (1). [D3, S3, F3]

4. **Tabular horns**. Directed posteriorly (0), posterolaterally (1), or laterally (2). [*D4, S4, F4*]

5. **Orbital margins**. Flush with plane of skull roof (0), or elevated above plane of skull roof (1). [D5, *S5*, F5]

6. **Postorbital-prepineal growth zone**. Absent (0), or present (1). [D6, S6, F6]

7. **Lateral line sulci**. Weakly impressed, discontinuous (0), or continuous, well impressed (1). [D7, S7, F7]

8. **Lacrimal flexure of infraorbital canal**. Absent (0), stepped (1), or Z-shaped (2). [D8, S8, F8]

9. **Occipital sensory canal**. Absent (0), or present (1). [D9, S9, F9]

10. **Supraorbital sensory canal**. Passes media to lacrimal (0), or enter lacrimal (1). [D10, *S10*, F10]

11. **Frontal**. Excluded from orbit (0), or entering medial margin of orbit. [D11, *S11*, F11]

12. **Supratemporal**. Entering dorsal margin of otic notch (0), or excluded from dorsal margin of otic notch (1). [D12, S12, F12]

13. **Preorbital projection of jugal**. Shorter than half the length of snout (0), or as long or longer (1). [*D13*, S13, *F13*]

14. **Postorbital**. Unexpanded (0), moderately antero-laterally expanded (1), or strongly anterolaterally expanded (2). [D14, *S14*, F14]

15. **Naris**. Oval (0), or narrow and elongated (1). [D15, S15, F15]

16. **Vomerine plate**. Short, as wide as long (0), or narrow and longer than wide (1). [*D16*, S16, *F16*]

17. **Occipital condyles**. Anterior to quadrate condyles (0), or level with or posterior to these (1). [D17, S17, F17]

18. **Choanal outline**. Oval-shaped (0), or narrow and slit-like (1), or circular (2). [D18, S18, F18]

19. **Transvomerine tooth row**. Transverse (0), or V-shaped (1). [D19, S19, F19]

20. **Anterior palatal vacuity**. Unpaired (0), or medially subdivided by anterior process (1), or completely subdivided (2). [*D20*, S20, *F20*]

21. **Pterygoid-parasphenoid suture**. As long as basal plate is wide (0), or

substantially longer than basal plate is wide (1). [*D21*, S21, *F21*]

22. **Cultriform process extension between vomers**. Extends beyond anterior margin of interpterygoid vacuities (0), or underplated by vomers (1). [D23, S23, F22]

23. **Cultriform process**. Ventrally flat (0), or flat with central ventral ridge (1), or slender with deep ventral crest ("knife edged") (2). [*D24*, S24, *F23*]

24. **Ectopterygoid**. Excluded from the lateral margin of interpterygoid vacuities (0), or entering margin, wedged between palatine and pterygoid (1). [*D25*, S25, *F24*]

25. **Crista muscularis, extension**. Behind posterior border of parasphenoid-pterygoid suture (0), or level with that border (1). [D26, S263, F25]

26. **Crista muscularis, midline**. Discontinuous (0), or confluent in midline (1). [D27, S27, F26]

27. **Parasphenoid pockets**. Facing posterodorsally, located along the posterior rim of the plate (0), or ventrally, entirely located on the flat surface (1). [D28, S28, F27]

28. **Exoccipital-pterygoid suture**. Absent (0), or present (1). [D29, S29, F28]

29. **Marginal teeth**. Circular or moderately oval (0), or anteroposteriorly compressed and closely set (1). [D30, S30, F29]

30. **Ectopterygoid tusks**. Present (0), or absent (1). [D31, S31, F30]

31. **Denticle field**. Present on parasphenoid and pterygoid (0), or absent (1). [D32, S32, F31]

32. **Quadratojugal**. Excluded from quadrate trochlea (0), or forming lateral portion of it (1). [D33, S33, F32]

33. **Posttemporal fenestra**. Narrow and slit-like (0), or triangular (1). [D35, S35,

F33]

34. **Tabular horn**. Short, supported only by paroccipital process (0), or posteriorly extended, supported by two ventral ridges (1). [*D36*, S36, *F34*]

35. **Crista obliqua of pterygoid**. Absent (0), or present (1). [D37, S37, F35]

36. **Crista muscularis of parasphenoid**. Visible in occipital view (0), or not visible (1). [D38, S38, F36]

37. **Basioccipital**. Present (0), or absent (1). [D39, S39, F37]

38. **Crista falciformis**. Absent (0), or present (1). [D40, S40, F38]

39. **Postglenoid area**. Short boss (0), or distinct process (1), or extended, longer than glenoid facet (2). [*D41*, S41, *F39*]

40. **Hamate process of prearticular**. Absent or rudimentary, forming at best an anterior margin of the glenoid facet (0), or present, raised well above glenoid and as high as quadrate trochlea (1), or substantially higher than quadrate trochlea (2). [*D42*, S42, *F40*]

41. **Posterior Meckelian fenestra**. Small and round (0), or elongated (1). [D43, S43, F39]

42. **Labial wall of adductor chamber**. Dorsally horizontal (0), or dorsally convex (1). [D44, S44, F42].

43. **Coronoid series**. With tooth patch (0), or single row of teeth (1). [D45, S45, F43]

44. **Prearticular**. Sutures with splenial anteriorly (0), or separated from it by dentary or coronoid 2 (1). [*D46*, S46, *F44*]

45. **Glenoid facet**. Above level of dorsal surface of dentary (0), or below (1). [D47,

S47, F45]

46. **Parietals and supratemporal length.** The parietal longer than the supratemporal (0), or similar in length (1). [*F46*]

47. **Postparietals and tabular length**. Shorter than parietals (0), or similar (1). [S53, *F47*]

48. **Interpterygoid vacuities**. Equally wide anteriorly and posteriorly (0), or basipterygoid ramus of the pterygoid is medially thickened and constricts the interpterygoid vacuities (1). [*S59,* F48]

49. P**osterior margin of the squamosal.** Straight or curved in a slightly convex manner (0), or forming a posteriorly extended plate that roofs the occiput (1). [F50]

50. **Postglenoid area**. Oblique dorsal and ventral margins (0), or straight dorsal margin bilaterally (1). [*F51*]

51. **Skull greatest width−to−midline length in adults**. 0.8–1.2 (0), <0.8 (1), >1.2 (2). [F52]

52. **Postorbital and prefrontal**. Widely separated (0), or nearing one another by thin projections (1), or sutured, excluding jugal from orbit margin (2). [S58, F53]

53. Otic fenestra. Tabular and squamosal separated by otic notch posteriorly (0), or separated by narrow slit (1), or sutured to encircle an otic fenestra (2). [S54].

54. **Palatine ramus of pterygoid**. Ventrally smooth (0), or ornamented (1). [S49]

55. Posterior boss of quadrate. Occipital face of quadrate with prominent posterior boss (0), or smooth (1). [S62]

56. **Cultriform process**. Merges continuously from basal plate (0), or forming a

deltoid base (1). [S51]